DOI: 10.1002/asia.200600069

Linking Chiral Clusters with Molybdate Building Blocks: From Homochiral Helical Supramolecular Arrays to Coordination Helices

De-Liang Long,[a] Paul Kögerler,[b] Louis J. Farrugia,[a] and Leroy Cronin*[a]

Abstract: The synthesis of four new oxo-centered Fe clusters (**1a–c**, **2**) of the form $[Fe^{III}_3(\mu_3\text{-}O)(CH_2{=}CHCOO)_6]$ with acrylate as the bridging ligand gives rise to potentially intrinsically chiral oxo-centered $\{M_3\}$ trimers that show a tendency to spontaneously resolve upon crystallization. For instance, **1a**, $[Fe^{III}_3(\mu_3\text{-}O)(CH_2{=}CHCOO)_6(H_2O)_3]^+$, crystallizes in the chiral space group $P3_1$ as a chloride salt. Crystallization of **1b**, $[Fe_3(\mu_3\text{-}O)(C_2H_3CO_2)_6(H_2O)_3]NO_3{\cdot}4.5H_2O$, from aqueous solution followed by recrystallization from acetonitrile also gives rise to spontaneous resolution to yield the homochiral salt $[Fe_3(\mu_3\text{-}O)(C_2H_3CO_2)_6(H_2O)_3]NO_3{\cdot}CH_3CN$ of **1c** (space group $P2_12_12_1$). Furthermore, the reaction of **1a** with hexamolybdate in acetonitrile gives the helical coordination polymer $\{[(Fe_3(\mu_3\text{-}O)L_6(H_2O))(MoO_4)(Fe_3(\mu_3\text{-}O)L_6(H_2O)_2)]{\cdot}2CH_3CN{\cdot}H_2O\}_\infty$ **2** (L: $H_2C{=}CHCOO$), which crystallizes in the space group $P2_1$. The nature of the ligand geometry allows the formation of atropisomers in both the discrete (**1a–c**) and linked $\{Fe_3\}$ clusters (**2**), which is described along with a magnetic analysis of **1a** and **2**.

Keywords: atropisomerism · crystal engineering · helical structures · polyoxometalates · supramolecular chemistry

Introduction

The control of molecular building blocks in the assembly of coordination or polyoxometalate clusters,[1] and control of the relative orientation of the clusters in a crystalline lattice, is of fundamental importance for the design of large and potentially functional architectures.[2] This is because a designed approach to the networking of discrete clusters is crucial for the synthesis of new materials with porosity,[3] novel magnetic,[4] chiral (including the ability to spontaneously resolve into chiral forms),[5] and optical properties.[6] A high level of control could also allow the emergence of new physics related to the ability to tune both the electronic and magnetic properties of discrete cluster units and intercluster interactions.[4–6] Nature also successfully adopts a building-block approach to the assembly of proteins by using a library of 20 amino acids, but a fundamental extra degree of control is gained by employing chiral building blocks.[7] The result is spectacular because folded proteins are normally observed to adopt one major folded architecture from countless possibilities.

Herein we report a route to form chiral cluster-based building blocks that can be connected in chains with molybdate building-block linkers. To develop this strategy, we built upon our synthetic approach to isolate novel polyoxomolybdate[8] and -tungstate[9] clusters by the use of large cations that "encapsulate" and kinetically stabilize otherwise reactive cluster anions.[8–10] The main questions were 1) if larger cations can be condensed with polyoxometalate (POM) clusters (or POM-based building blocks) to form new architectures and 2) if cations with additional functionality can be utilized (e.g., with electrochemical,[5] optical,[6] magnetic, or chiral properties) to modify the properties of the overall cluster network.

A simple and stable cationic system that can address these questions is based on the well-known family of μ_3-oxo-centered and carboxylate-bridged trimeric $\{Fe_3\}$ clusters of the type $[Fe_3(\mu_3\text{-}O)(\mu_2\text{-}O_2CR)_6]^+ = \{Fe_3OL_6\}^+$.[11] Historically, these species have been of great interest owing to their magnetic[12] and electronic[13] proprieties since they were characterized more than 60 years ago. Work has focused on the intramolecular electron-transfer process of mixed-valence Fe^{II}/Fe^{III} derivatives[11–13] of such trimers, and a few examples of polymeric $\{Fe_3OL_6\}$ structures have been reported

[a] Dr. D.-L. Long, Dr. L. J. Farrugia, Prof. L. Cronin
WestCHEM, Department of Chemistry
The University of Glasgow
Glasgow, G12 8QQ (UK)
Fax: (+44) 141-330-4888
E-mail: L.Cronin@chem.gla.ac.uk

[b] Dr. P. Kögerler
Ames Laboratory and Department of Physics and Astronomy
Iowa State University
Ames, IA 50011 (USA)

in which the networks are based on supramolecular interactions, but very rarely with covalent bonds.[14]

Results and Discussion

We opted herein to expand the structural variety of such trimeric clusters by introducing acrylate as a bridging ligand, here assigned as L. Once these are coordinated to the $\{Fe_3O\}$ core, the relative orientation of the six vinyl residues is locked; they are coplanar with the chelated carboxylate moiety owing to π-electron delocalization, with a rotation energy barrier of about 26 kJ mol^{-1} between the two possible clockwise or anticlockwise orientations.[15] This means that each $\{Fe_3OL_6\}^+$ cluster has $2^6=64$ possible configurations in the solid state. Geometrical analysis of these configurations differentiates 16 distinct isomers that define nine potential atropisomers[16] (α, β, γ_{1-3}, δ_{1-4}; Figure 1), seven of which (β, $\gamma_{2,3}$, δ_{1-4}) are chiral. As such, the use of acrylate ligands could result in the first examples of intrinsically chiral oxo-centered M_3 trimers.[17] Indeed, we realized the potential of producing such chiral cations with the synthesis of the $[Fe^{III}_3(\mu_3\text{-}O)(CH_2{=}CHCOO)_6(H_2O)_3]^+$ cation (**1**), which undergoes spontaneous resolution and crystallizes in the chiral space group $P3_1$ as a chloride salt $[Fe_3(\mu_3\text{-}O)(C_2H_3CO_2)_6(H_2O)_3]Cl{\cdot}7H_2O$ (**1a**). Only pure δ_2* and γ_2* enantiomers are found in the solid-state structure of **1a**. We suggest that this observed homochirality is related to the fact that all three chiral cluster cations present in the asymmetric unit of **1a** adopt chiral atropisomers. In contrast, the corresponding nitrate salt $[Fe_3(\mu_3\text{-}O)(C_2H_3CO_2)_6(H_2O)_3]NO_3{\cdot}4.5H_2O$ (**1b**) contains a racemic mixture of both enantiomers of the δ_3 isomer and, thus, is not formed as a homochiral compound. However, spontaneous resolution is again observed if **1b** is recrystallized from acetonitrile to yield the homochiral salt $[Fe_3(\mu_3\text{-}O)(C_2H_3CO_2)_6(H_2O)_3]NO_3{\cdot}CH_3CN$ (**1c**), which contains an enantiomerically pure δ_2 isomer. This isomer is the mirror image of the δ_2* enantiomer found in **1a**; compound **1c** crystallizes in the chiral space group $P2_12_12_1$.

We also report the reaction of **1a** with hexamolybdate in acetonitrile to give the helical coordination polymer $\{[(Fe_3(\mu_3\text{-}O)L_6(H_2O))(MoO_4)(Fe_3(\mu_3\text{-}O)L_6(H_2O)_2)]{\cdot}2CH_3CN{\cdot}H_2O\}_\infty$ (**2**; L = H$_2$C=CHCOO), which contains enantiomerically pure δ_3 and δ_4 isomers. Compounds **1a** and **1b** were obtained as red crystals upon solvent evaporation of an aqueous solution of sodium acrylate and iron(III) chloride or iron(III) nitrate, respectively (2:1). Compounds **1a**, **1b**, **1c**, and **2** were characterized by single-crystal X-ray crystallography (Table 1), and **1a**, **1b**, and **2** were further characterized by elemental analysis, IR and UV/Vis spectroscopy, and magnetic measurements (data for **1a** and **2** are presented here).

The single-crystal X-ray crystallographic analyses reveal that **1a** comprises the typical trigonal-planar $\{Fe_3(\mu_3\text{-}O)\}$ core fragment (Figure 2). Fe–(μ_3-O) bond lengths range from 1.895(3) to 1.917(3) Å, and Fe–Fe distances from 3.274(1) to 3.321(1) Å. The asymmetric unit consists of three

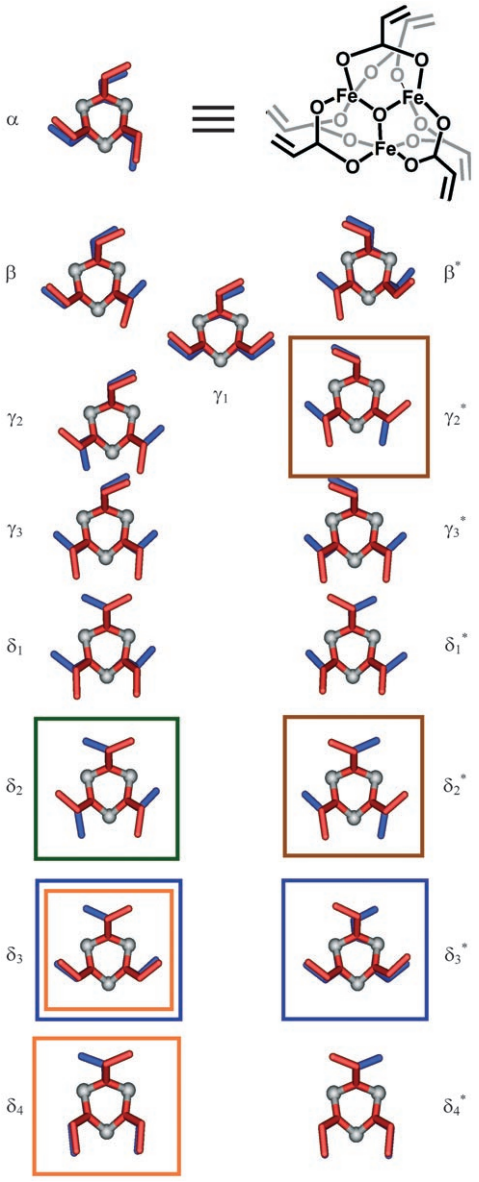

Figure 1. A schematic representation of the absolute configurations of all 16 unique isomers of the $\{Fe_3OL_6\}$ cluster cations, α, β, γ_{1-3}, δ_{1-4} (a structural representation of the α isomer is also given, top right, for clarity).[16b] The rear acrylate ligands are in blue and the frontal ones in red, Fe centers are the grey spheres, and the oxygen atoms of the ligand are omitted so that the orientation of the vinyl group is highlighted. Colored boxes are used to identify the actual isomers found in the presented compounds. Isomers found in **1a** are highlighted by brown, **1b** by blue, **1c** by green, and **2** by orange boxes. Note that **1b** contains a racemic mixture of both the δ_3* and δ_3 enantiomers.

independent cluster cations, each with distinct geometries and slightly different Fe–Fe distances and Fe–O bond lengths, which results in nine cluster cations in the unit cell (Figure 2). Besides the central oxo ligand, every pair of iron centers is linked by two acrylate bridges whereby the carboxylate planes and the Fe_3O planes form dihedral angles of 41 to 54°. A water ligand coordinates to each Fe center, positioned *trans* to the μ_3-oxo center, to complete the slightly distorted octahedral coordination environment.

Table 1. Crystallographic data for complexes **1a–c** and **2**.

	1a	**1b**	**1c**	**2**
Formula	$C_{18}H_{24}ClFe_3O_{16}\cdot 7H_2O$	$C_{18}H_{24}Fe_3N_3O_{19}\cdot 4.5H_2O$	$C_{18}H_{24}Fe_3NO_{19}\cdot CH_3CN$	$C_{36}H_{42}Fe_6MoO_{39}\cdot H_2O\cdot(CH_3CN)_2$
M_r [g mol^{-1}]	825.48	807.00	766.99	1533.86
Crystal system	trigonal	monoclinic	orthorhombic	monoclinic
Space group	$P3_1$	$P2_1/c$	$P2_12_12_1$	$P2_1$
a [Å]	29.2906(2)	12.5532(2)	12.6314(4)	13.0808(5)
b [Å]	29.2906(2)	15.5922(3)	14.1659(8)	14.5819(8)
c [Å]	10.2986(1)	16.0622(3)	17.1485(10)	16.4911(9)
β [°]	90	90.839(1)	90	112.543(3)
V [Å^3]	7561.83(10)	3143.55(10)	3068.5(3)	2905.2(3)
ρ_{calcd} [g cm^{-3}]	1.612	1.705	1.660	1.753
Z	9	4	4	2
μ ($Mo_{K\alpha}$) [mm^{-1}]	1.426	1.461	1.483	1.761
T [K]	100(2)	200(2)	120(2)	150(2)
No. reflections (meas)	80314	23051	13471	21017
No. reflections (indep)	19884	6182	6011	8804
No. reflections (obs)	19429	4991	4845	6792
No. params	1216	459	416	749
$R1$ ($I>2\sigma(I)$)	0.0338	0.0363	0.0404	0.0656
$wR2$ (all data)	0.0840	0.0844	0.0814	0.1666

Figure 1 shows the absolute configurations of the two discrete enantiomers found in **1a** (two of the three crystallographically independent cations are of the same γ_2* conformation). Their presence results in an interesting solid-state structure with chiral configurations of counterion–solvent (Cl^-/H_2O here) channels. Hexagonal arrangements of the chiral $\{Fe_3OL_6\}^+$ cations are supported by weak intermolecular interactions; in particular, the intermolecular interactions between the acrylate ligands (π···π, CH···π, CH···OC) of adjacent clusters facilitates the assembly of helical arrangements of both anions and solvent in the channels of **1a**, which run parallel to the crystallographic *c* axis (Figure 2). Similar but nonchiral ion channels are also present in the crystal lattice of the nitrate salt **1b** (space group $P2_1/c$). Here, a racemic mixture of $\{Fe_3OL_6\}^+$ (δ_3 isomers) borders these channels from four sides. In contrast, only one δ_2 enantiomer is found in the recrystallized compound **1c**, in which the planar $\{Fe_3O\}$ group is parallel to the crystallographic *ab* plane.

Compound **2** was assembled by linking the cations found in **1a** with $[MoO_4]^{2-}$ derived from $(Bu_4N)_2[Mo_6O_{19}]$ in acetonitrile (Figure 3). The use of a nonaqueous solvent and $(Bu_4N)_2[Mo_6O_{19}]$ as a source of molybdate proved to be crucial for the production of **2**; reaction of an aqueous solution of $\{Fe_3O\}$-type cations with sodium molybdate quickly produced an amorphous precipitate.

The slow decomposition of the $[Mo_6O_{19}]^{2-}$ anion in acetonitrile to $[MoO_4]^{2-}$, the linking molybdate moiety found in **2**, appears to be the rate-determining step in the crystallization of **2**. During the assembly process, water ligands coordinated to $\{Fe_3OL_6\}^+$ are removed and replaced by molybdate oxo ligands. Compound **2** is based on helical strands of a coordination polymer propagating along the crystallographic *b* axis (Figure 3; **2** crystallizes in the space group $P2_1$). The helix consists of tetrahedral $[MoO_4]^{2-}$ groups that coordinate to two types of $\{Fe_3OL_6\}^+$. The first, "bridging" δ_3-$\{Fe_3OL_6\}^+$ trimer replaces two of its three H_2O ligands and binds to two neighboring molybdate groups (Fe–Mo: 3.681(2) and 3.730(3) Å) to form the –Mo–Fe–Fe–Mo–Fe–Fe– backbone of the helix. The second, "side-on" δ_4-$\{Fe_3OL_6\}^+$ trimer binds to one of the two remaining uncoordinated oxo positions of the molybdate group, which in turn replaces one of the three H_2O ligands of the trimer

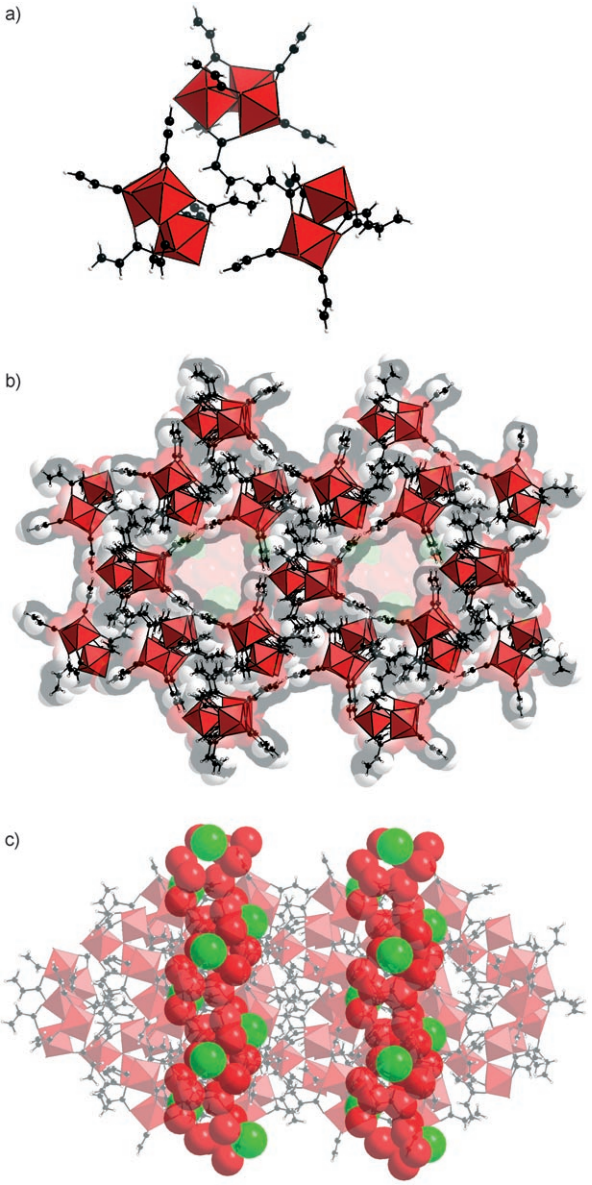

Figure 2. a) The asymmetric unit of **1a** comprising three $\{Fe_3OL_6\}$ cations. b) This view shows how these units aggregate to form hexagonal ion–solvent channels. c) A view of the solvent within these channels, in which the ions and solvent form hydrogen-bonded helices. $\{Fe_3O\}$ units are shown as red polyhedra, carbon and hydrogen atoms are in black and white, respectively, and the oxygen and chloride positions are emphasized as red and green spheres, respectively.

CHEMISTRY
AN ASIAN JOURNAL

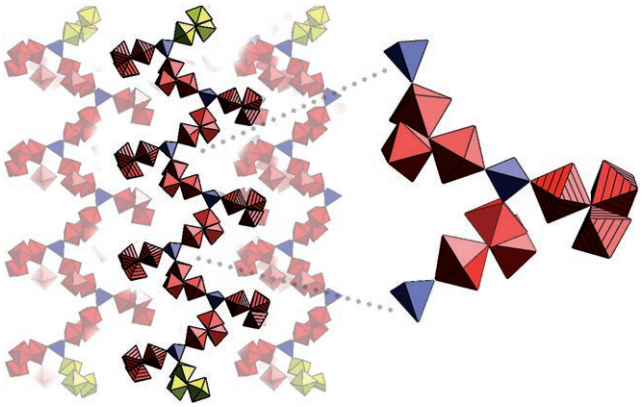

Figure 3. Polyhedral plot of the helical polymer in **2** with a subsection enlarged. Blue tetrahedra represent molybdates, red corner-sharing octahedra show the bridging $\{Fe_3\}$ groups, red striped octahedra are the "end-on" $\{Fe_3\}$ groups, and yellow polyhedra represent the end of each strand shown.

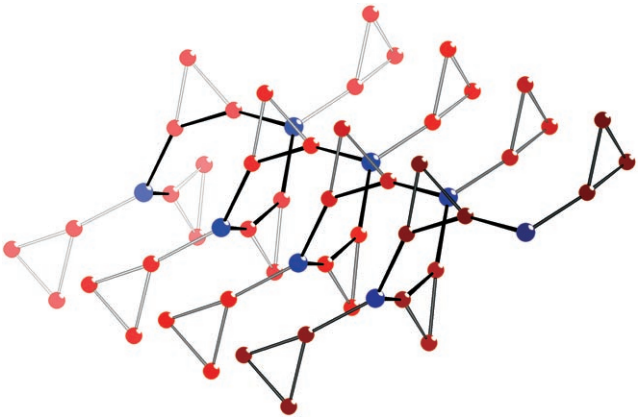

Figure 4. The metal skeleton of a section of a helical strand in **2** (Mo: blue, Fe: red) illustrating the alternating orientation of the "end-on" δ_4-$\{Fe_3\}$ groups.

(Fe–Mo: 3.515(7) Å). This results in the helical arrangement of the polymer strand, in which the sequence molybdate–bridging $\{Fe_3O\}$ trimer–molybdate–bridging $\{Fe_3O\}$ trimer defines one pitch (repeat unit) of the helix (Figure 4) and extends it by 14.58 Å along its axis. With regard to this axis, the side-on $\{Fe_3O\}$ groups are oriented nearly perpendicular, and consecutive side-on groups are positioned *trans* to each other. Three of the four oxo ligands of the $[MoO_4]$ moiety coordinate to different $\{Fe_3OL_6\}^+$ trimers with Mo–O bond lengths of 1.767(9), 1.796(8) (to bridging $\{Fe_3O\}$), and 1.853(7) Å (to side-on $\{Fe_3OL_6\}^+$); the remaining terminal oxo position shows a Mo=O double bond of length 1.675(7) Å. The Fe–O(Mo) bond lengths are 1.976(8), 1.989(8), and 2.011(8) Å, respectively. Whereas the Fe–O–Mo bond angles involving the bridging $\{Fe_3OL_6\}^+$ groups are widened (154.79°/161.71°), the side-on Fe–O–Mo bond angle is lowered to 132.43°. The coordination to the molybdate groups barely affects the geometry of the $\{Fe_3OL_6\}^+$ moiety (Fe–(μ_3-O) vectors: 1.875(7) to 1.946(7) Å (bridging) and 1.883(10) to 1.958(8) Å (side-on)). The solvent molecules act as spacers between neighboring helical strands in the crystal lattice with closest interhelix Fe–Fe contacts of 5.34 Å.

The magnetic properties of the monomeric $\{Fe_3OL_6\}^+$ compound **1a** are characterized by intramolecular antiferromagnetic exchange between the $s = {}^5/_2$ Fe^{III} centers. The spin array of all three $\{Fe_3OL_6\}$ isomers in **1a** was simplified to an isosceles triangle. A least-squares fit of an isotropic Heisenberg model with a spin Hamiltonian $H = -(J_A S_1 S_2 + J_B S_1 S_3 + J_C S_2 S_3)$ to the experimental susceptibility data (2–290 K) yields $J_A/k_B = -37.7$ K, $J_B/k_B = -37.7$ K, and $J_C/k_B = -45.4$ K, with a common g factor of $g_{iso} = 1.99$ and a total ground state of $S = {}^1/_2$ (Figure 5a). These exchange constants, two smaller and nearly identical and one larger, are in good agreement with values reported for similar car-

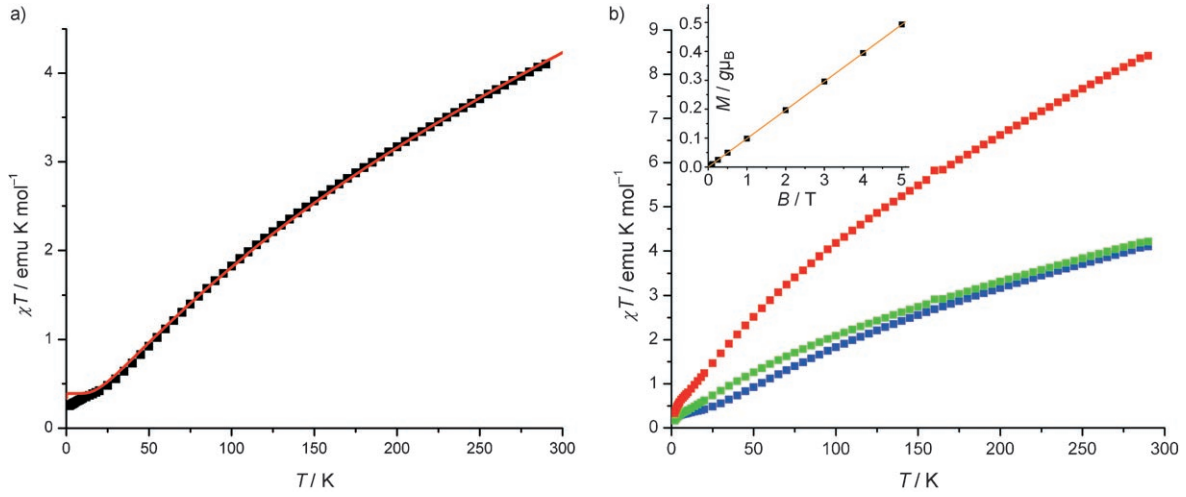

Figure 5. a) Temperature dependence of χT for **1a** at 0.1 T. ■ = Experimental and corrected for diamagnetic contributions, —— = best fit for Heisenberg model for a spin triangle employing three exchange constants. b) Temperature dependence of χT at 0.1 T. ■ = Helical $\{Fe_6Mo_2\}$ polymer **2**, ■ = molar susceptibility data of **2** referenced to half the molecular mass of the monomer unit, effectively referring to one $\{Fe_3\}$ triangle per formula unit, ■ = discrete $\{Fe_3\}$ cluster **1**. Inset: Plot of magnetization versus field for **2** at 2.0 K. ■ = Experimental, —— = linear least-squares fit illustrating the linearity of M versus B, which indicates the absence of magnetic impurities and the singlet ground state of **2**.

boxylate-based $\{Fe_3OL_6\}$ clusters[11d] and correspond to a near-perfect isosceles Fe_3 triangle despite the observed minor differences in the Fe–Fe distances. The observed deviation below about 7 K from the calculated χT curve, which approaches a value of 0.35 emu K mol^{-1}, can be attributed to intermolecular coupling that stems from the close contact of some vinyl groups to the terminal oxo positions of neighboring $\{Fe_3\}$ molecules.

Linking the $\{Fe_3\}$ units to the polymeric helix structure **2**, however, complicates the magnetic analysis due to the presence of three different Fe–O–Mo–O–Fe and six different Fe–O–Fe contacts, although the isosceles-triangular shape of both the end-on and the helix backbone $\{Fe_3\}$ triangles, in a first approximation, should reduce this to four types of Fe–O–Fe contacts. As with **1a**, the measured susceptibility of **2** displays strong antiferromagnetic exchange coupling. However, if the molar susceptibility is scaled to represent a single $\{Fe_3Mo\}$ unit, a direct comparison with the discrete $\{Fe_3\}$ compound shows similar features: χT displays a shoulder at around 10 K (around 15 K for $\{Fe_3\}$) and a nearly identical slope above 150 K (Figure 5b). In a first approximation, this finding indicates that the magnetic properties of the helix compound **2** are dominated by intratriangle coupling similar to that of the isolated $\{Fe_3\}$ species **1a**, whereas the coupling between neighboring triangles via the molybdate bridges is weaker and, therefore, causes deviations in the χT versus T curves only for lower temperatures (<120 K).

Conclusions

The formation of a surprising chiral helix from molybdate anions and $\{Fe_3OL_6\}$-type cations illustrates the potential of stable polynuclear complexes to act as functional transferable building blocks in the construction of coordination networks. The observation of spontaneous resolution to yield chiral crystalline products of isolated cluster units and helical polymers due to atropisomerism is interesting.[18] It would appear that rapid locking of the vinyl groups upon crystallization can be compared to a type of conformational funnelling from all possible configurations to the winning outcome. If the assembly process presented herein can be understood, and the building blocks be predictably transformed, it will allow the design of materials that can reliably undergo spontaneous resolution; this could lead to the design of new materials with exotic optical, electronic, and magnetic properties as well as access to complex molecular and network structures. The terminal vinyl groups also present a further target for coupling reactions involving **1a**. We will pursue such studies in forthcoming work along with attempts to synthesize cluster receptors decorated with acrylate, as such systems, with potentially billions of isomers, could be utilized in a new type of supramolecular host–guest interaction whereby the host is selected from a dynamic conformational library based on atropisomers.

Experimental Section

Syntheses

1a: $FeCl_3{\cdot}6H_2O$ (10.8 g, 40 mmol) was dissolved in water (100 mL). A solution of acrylic acid (5.6 mL, 82 mmol) and $NaOCH_3$ (4.2 g, 78 mmol) in water (50 mL) was added with stirring. The dark-red solution was heated to 70 °C for 1 h (pH ≈ 1.3). After cooling, the solution was filtered and the filtrate was kept in an open flask for a week, after which dark-red crystals of **1a** were isolated (4.8 g, 44 %). UV/Vis: $\lambda_{max} \approx 354$ nm (sh); IR (KBr disc): $\tilde{\nu}$ = 3397, 1642, 1577 (ν_{as}(COO)), 1437 (ν_s(COO)), 1372, 1277, 1070, 987, 828, 670, 564 cm^{-1} (ν_{as}(Fe_3O)); elemental analysis: calcd (%) for $C_{18}H_{38}ClFe_3O_{23}$: C 26.19, H 4.64; found: C 26.07, H 3.51 %.

1b: $Fe(NO_3)_3{\cdot}9H_2O$ (24.1 g, 59.6 mmol) was dissolved in water (200 mL). A solution of acrylic acid (8.4 mL, 123 mmol) and $NaOCH_3$ (6.0 g, 111 mmol) in water (10 mL) was added with stirring. The dark-red solution was kept in an open flask for a week, after which dark-red crystals of **1b** were isolated (6.4 g, 40 %). UV/Vis: $\lambda_{max} \approx 350$ nm (sh); IR (KBr disc): $\tilde{\nu}$ = 3430, 1641, 1570, 1438, 1383, 1276, 1069, 987, 829, 670, 618 cm^{-1}; elemental analysis: calcd (%) for $C_{18}H_{33}Fe_3NO_{23.5}$: C 26.8, H 4.1, N 1.7; found: C 26.8, H 3.9, N 1.8 %.

1c: **1b** (1.6 g, 2 mmol) and $(Bu_4N)_2Mo_6O_{19}$ (0.50 g, 0.36 mmol) were dissolved in CH_3CN (40 mL). Upon evaporation, a few crystals of **1c** were formed next to a large amount of amorphous precipitate.

2: **1a** (0.56 g, 0.68 mmol) and $(Bu_4N)_2[Mo_6O_{19}]$ (0.40 g, 0.29 mmol) were dissolved in acetonitrile (25 mL). The resulting red solution was filtered and sealed in a vial. Red crystals appeared after 10 days (0.13 g, 25 %). UV/Vis: $\lambda_{max} \approx 338$ nm (sh); IR (KBr disc): $\tilde{\nu}$ = 3425, 1643, 1575, 1437, 1372, 1274, 1069, 990, 890, 830, 778, 670, 537 cm^{-1}; elemental analysis: calcd (%) for $C_{40}H_{50}Fe_6MoN_2O_{34}$: C 31.32, H 3.29, N 1.83; found: C 31.40, H 3.27, N 1.94 %.

X-ray Crystallographic Studies of the Complexes

Data were measured at 100–200(2) K on a Nonius KappaCCD diffractometer ($\lambda(Mo_{K\alpha}) = 0.71073$ Å) with a graphite monochromator. Structure solution was performed with SHELXS-97 and refinement with SHELXL-97 through WINGX.[19] CCDC 286771–286774 contain the supplementary crystallographic data for **1a, 1b, 1c**, and **2**, respectively. These data can be obtained free of charge from the Cambridge Crystallographic Data Centre, 12, Union Road, Cambridge CB2 1EZ, UK (fax: (+44) 1223-336-033; email: deposit@ccdc.cam.ac.uk) or at www.ccdc.cam.ac.uk/conts/retrieving.html.

Magnetic Studies

Magnetic susceptibility measurements were performed at 0.1 and 5.0 T with a Quantum Design MPMS-5 SQUID magnetometer. Data were corrected for diamagnetic and temperature-independent paramagnetic (TIP) contributions ($\chi_{dia/TIP}$(**1a**) = -478×10^{-6} emu mol^{-1}, $\chi_{dia/TIP}$(**2**) = -640×10^{-6} emu mol^{-1}). Field-dependent measurements at various low temperatures confirmed the $S = 1/2$ ground state for **1a** (reproducing the expected Brillouin function) and the $S = 0$ ground state for **2**, as well as the absence of significant amounts of magnetic impurities in both samples. Further studies on **2** will be reported later.

Acknowledgements

This work was supported by the Leverhulme Trust (London), the Royal Society, the University of Glasgow, and the EPSRC. Ames Laboratory is operated for the U.S. Department of Energy by Iowa State University under Contract No. W-7405-Eng-82.

[1] a) A. Müller, F. Peters, M. T. Pope, D. Gatteschi, *Chem. Rev.* **1998**, *98*, 239; b) A. Müller, S. Roy, *Coord. Chem. Rev.* **2003**, *245*, 153.

[2] a) D. Braga, *Chem. Commun.* **2003**, 2751; b) D. Braga, L. Brammer, N. R. Champness, *CrystEngComm* **2005**, *7*, 1; c) D. Braga, F. Grepio-

ni, *Angew. Chem.* **2004**, *114*, 4092; *Angew. Chem. Int. Ed.* **2004**, *43*, 4002.

[3] a) M. Eddaoudi, D. B. Moler, H. Li, B. Chen, T. M. Reineke, M. O'Keeffe, O. M. Yaghi, *Acc. Chem. Res.* **2001**, *34*, 319; b) A. J. Blake, N. R. Champness, R. Hubberstey, W. S. Li, M. A. Withersby, M. Schroder, *Coord. Chem. Rev.* **1999**, *183*, 117; c) W. Lin, *J. Solid State Chem.* **2005**, *178*, 2486; d) K. Biradha, C. Seward, M. J. Zaworotko, *Angew. Chem.* **1999**, *111*, 584; *Angew. Chem. Int. Ed.* **1999**, *38*, 492.

[4] a) A. Müller, A. M. Todea, J. Slageren, M. Dressel, H. Bögge, M. Schmidtmann, M. Luban, L. Engelhardt, M. Rusu, *Angew. Chem.* **2005**, *117*, 3925; *Angew. Chem. Int. Ed.* **2005**, *44*, 3857; b) A. Müller, M. Luban, C. Schröder, R. Modler, P. Kögerler, M. Axenovich, J. Schnack, P. Canfield, S. Bud'ko, N. Harrison, *ChemPhysChem* **2001**, *2*, 517.

[5] a) X. Fang, T. M. Anderson, C. L. Hill, *Angew. Chem.* **2005**, *117*, 3606; *Angew. Chem. Int. Ed.* **2005**, *44*, 3540; b) U. Siemeling, I. Scheppelmann, B. Neumann, A. Stammler, H.-G. Stammler, J. Frelek, *Chem. Commun.* **2003**, 2236; c) V. Balamurugan, R. Mukherjee, *CrystEngComm* **2005**, *7*, 337; d) L. Perez-Garcia, D. B. Amabilino, *Chem. Soc. Rev.* **2002**, *31*, 342.

[6] T. Yamase, *Chem. Rev.* **1998**, *98*, 307.

[7] E. Alm, D. Baker, *Proc. Natl. Acad. Sci. USA* **1999**, *96*, 11305.

[8] D.-L. Long, P. Kögerler, L. J. Farrugia, L. Cronin, *Angew. Chem.* **2003**, *115*, 4312; *Angew. Chem. Int. Ed.* **2003**, *42*, 4180.

[9] D.-L. Long, H. Abbas, P. Kögerler, L. Cronin, *J. Am. Chem. Soc.* **2004**, *126*, 13880.

[10] a) D.-L. Long, P. Kögerler, L. J. Farrugia, L. Cronin, *Angew. Chem.* **2004**, *116*, 1853; *Angew. Chem. Int. Ed.* **2004**, *43*, 1817; b) D.-L. Long, D. Orr, G. Seeber, P. Kögerler, L. Farrugia, L. Cronin, *J. Cluster Sci.* **2003**, *14*, 313.

[11] a) A. K. Boudalis, Y. Sanakis, C. P. Raptopoulou, A. Terzis, J. P. Tuchagues, S. P. Perlepes, *Polyhedron* **2005**, *24*, 1540; b) A. Bino, I. Shweky, S. Cohen, E. R. Bauminger, S. J. Lippard, *Inorg. Chem.* 1998, 37, 5168; c) C. Serre, F. Millange, S. Surble, G. Ferey, *Angew. Chem.* **2004**, *116*, 6445; *Angew. Chem. Int. Ed.* **2004**, *43*, 6286.

[12] a) J. Overgaard, F. K. Larsen, B. Schiott, B. B. Iversen, *J. Am. Chem. Soc.* **2003**, *125*, 11088; b) R. W. Wu, M. Poyraz, F. E. Sowrey, C. E. Anson, S. Wocadlo, A. K. Powell, U. A. Jayasooriya, R. D. Cannon, T. Nakamoto, M. Katada, H. Sano, *Inorg. Chem.* **1998**, *37*, 1913.

[13] F. E. Sowrey, C. Tilford, S. Wocadlo, C. E. Anson, A. K. Powell, S. M. Bennington, W. Montfrooij, U. A. Jayasooriya, R. D. Cannon, *J. Chem. Soc. Dalton Trans.* **2001**, 862.

[14] a) A. K. Boudalis, Y. Sanakis, C. P. Raptopoulou, A. Terzis, J. P. Tuchagues, S. P. Perlepes, *Polyhedron* **2005**, *24*, 1540; b) for a nice example of the condensation of $\{Fe_3O\}$ clusters with phosphonates to form discrete clusters, see: E. I. Tolis, M. Helliwell, S. Langley, J. Raftery, R. E. P. Winpenny, *Angew. Chem.* **2003**, *115*, 3934; *Angew. Chem. Int. Ed.* **2003**, *42*, 3804.

[15] The energy barrier between the two orientations of the vinyl residue of one of the six acrylate ligands was determined from density functional theory calculations on a (closed-shell) $[Ga_3O(CH_2{=}CH{-}COO)_6]^+$ model compound by a systematic variation of the C–C–C–O torsion angle. The model compound was constructed by adopting the crystallographic coordinates of the $\{Fe_3OL_6\}$ δ_2 isomer and relaxing this structure as $\{Ga_3OL_6\}$. This unconstrained geometry optimization resulted in maximal heavy-atom shifts smaller than 0.14 Å. Different transitional geometries with modified torsion angles were derived from this relaxed geometry to identify the barrier for a 180° flip. Calculations with the TURBOMOLE 5.7 package (O. Treutler, R. Ahlrichs, *J. Chem. Phys.* **1995**, *102*, 346) employed TZVP basis sets and hybrid B3-LYP exchange-correlation functionals.

[16] *Stereochemistry of Carbon Compounds* (Ed: E. L. Eliel), New York, McGraw-Hill, **1962**, pp. 156–178. Isomer definition: in the α isomer, the orientation of the vinyl residues of all six ligands are identical (*syn*), whereas in the β isomers, one $HC{=}CH_2$ terminal has a different (*anti*) orientation from the other five. In the γ and δ isomers, two and three terminals are *anti* from the other four and three, respectively. All possible mirror images of the symmetric enantiomers are indicated by the asterisk.

[17] To our knowledge, there are no intrinsically chiral oxo-centered M_3 trimers that incorporate achiral ligands, although one interesting example of a trimer system with a chiral ligand has been reported; see: a) J. S. Seo, D. Whang, H. Lee, S. I. Jun, J. Oh, Y. J. Jeon, K. Kim, *Nature* **2000**, *404*, 982; there is also one example of a cluster incorporating an amino acid; see: b) R. V. Thundathil, E. M. Holt, S. L. Halt, K. J. Watson, *J. Am. Chem. Soc.* **1977**, *99*, 1818.

[18] M. Vestergren, A. Johansson, A. Lennartson, M. Hakansson, *Mendeleev Commun.* **2004**, 258.

[19] L. J. Farrugia, *J. Appl. Crystallogr.* **1999**, *32*, 837.

Received: March 13, 2006
Published online: August 25, 2006

